iScience

CellPress OPEN ACCESS

Article

Intranasal murine pneumonia virus-vectored SARS-CoV-2 vaccine induces mucosal and serum antibodies in macaques

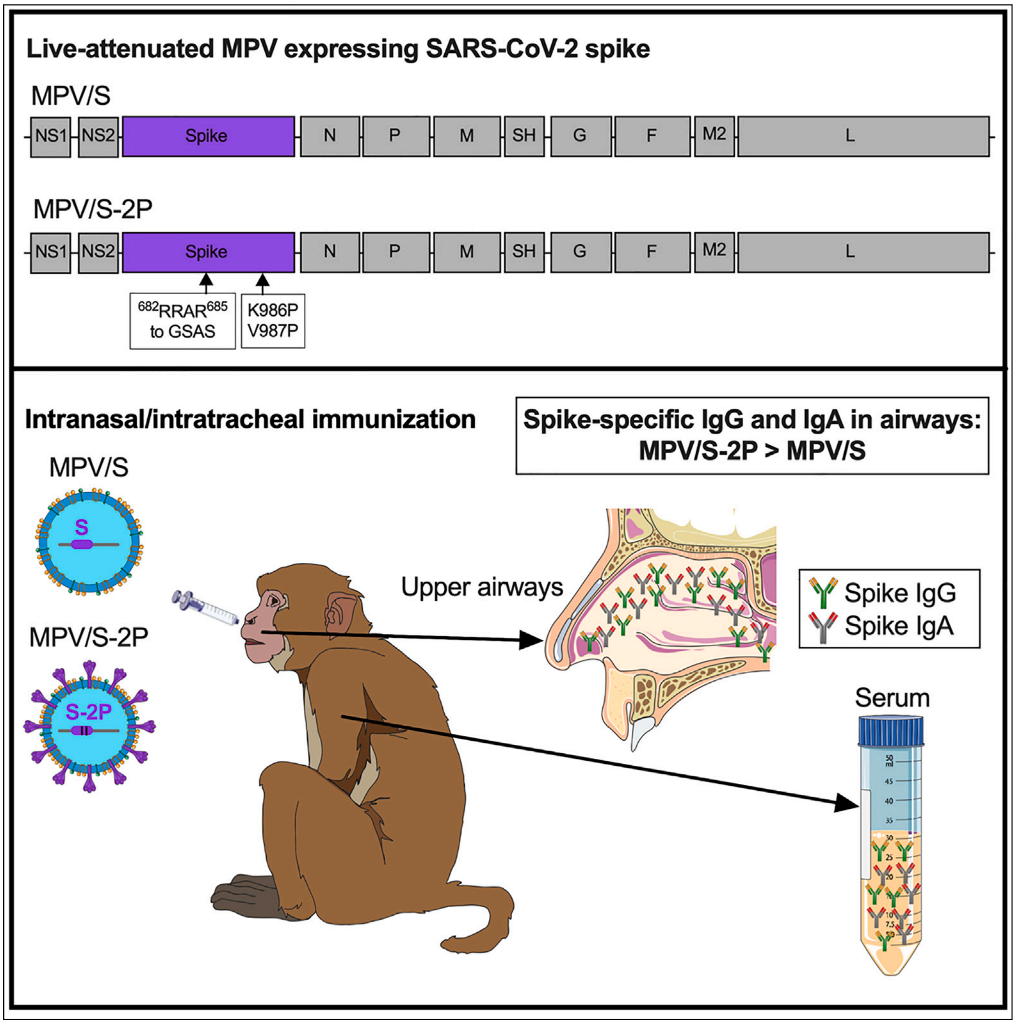

Jaclyn A. Kaiser, Xueqiao Liu, Cindy Luongo, ..., Shirin Munir, Cyril Le Nouën, Ursula J. Buchholz

ubuchholz@niaid.nih.gov

Highlights

Murine pneumonia virus (MPV) was used as a vector to express SARS-CoV-2 spike protein

Macaques were immunized by the respiratory mucosal route with MPV/S or MPV/S-2P

MPV/S-2P induced strong mucosal and serum anti-spike antibody responses in macaques

MPV/S-2P will be evaluated as a live-attenuated intranasal COVID-19 vaccine

Kaiser et al., iScience *26*, 108490
December 15, 2023
https://doi.org/10.1016/j.isci.2023.108490

iScience

CellPress
OPEN ACCESS

Article

Intranasal murine pneumonia virus-vectored SARS-CoV-2 vaccine induces mucosal and serum antibodies in macaques

Jaclyn A. Kaiser,[1] Xueqiao Liu,[1] Cindy Luongo,[1] Yumiko Matsuoka,[1] Celia Santos,[1] Lijuan Yang,[1] Richard Herbert,[2] Ashley Castens,[2] David W. Dorward,[3] Reed F. Johnson,[4] Hong-Su Park,[1] Sharmin Afroz,[1] Shirin Munir,[1] Cyril Le Nouën,[1] and Ursula J. Buchholz[1,5,*]

SUMMARY

Next-generation SARS-CoV-2 vaccines are needed that induce systemic and mucosal immunity. Murine pneumonia virus (MPV), a murine homolog of respiratory syncytial virus, is attenuated by host-range restriction in nonhuman primates and has a tropism for the respiratory tract. We generated MPV vectors expressing the wild-type SARS-CoV-2 spike protein (MPV/S) or its prefusion-stabilized form (MPV/S-2P). Both vectors replicated similarly in cell culture and stably expressed S. However, only S-2P was associated with MPV particles. After intranasal/intratracheal immunization of rhesus macaques, MPV/S and MPV/S-2P replicated to low levels in the airways. Despite its low-level replication, MPV/S-2P induced high levels of mucosal and serum IgG and IgA to SARS-CoV-2 S or its receptor-binding domain. Serum antibodies from MPV/S-2P-immunized animals efficiently inhibited ACE2 receptor binding to S proteins of variants of concern. Based on its attenuation and immunogenicity in macaques, MPV/S-2P will be further evaluated as a live-attenuated vaccine for intranasal immunization against SARS-CoV-2.

INTRODUCTION

Severe acute respiratory syndrome coronavirus 2 (SARS-CoV-2) emerged in late 2019 and has been a worldwide public health burden since early 2020.[1,2] SARS-CoV-2 is the causative agent of coronavirus infectious disease (COVID-19), which predominantly causes disease of the respiratory tract, though other symptoms can also occur.[3,4]

mRNA-based COVID-19 vaccines became available under emergency use authorization (EUA) in late 2020, and a non-replicating adenovirus-vector-based vaccine as well as a protein subunit vaccine were authorized under EUA shortly thereafter.[5–9] These COVID-19 vaccines were effective in reducing the burden of severe COVID-19 and COVID-19 mortality.[10] However, these injectable vaccines do not directly stimulate immunity in the respiratory mucosa, and booster immunizations are required to maintain protection. Furthermore, current COVID-19 vaccines are not highly effective in preventing infection and replication of SARS-CoV-2 at the respiratory mucosal entry sites; transmission rates remain high, allowing for the continued emergence of new variants. SARS-CoV-2 vaccines are needed that induce a robust mucosal immune response.[11,12]

Here, we used murine pneumonia virus (MPV) as a viral vector to express the SARS-CoV-2 spike (S) protein. MPV is the murine homolog of respiratory syncytial virus (RSV) and there is no or minimal pre-existing immunity to MPV in humans.[13] Our group previously evaluated MPV as a vector to express the RSV fusion (F) protein. We found that MPV was suitable for stable expression of a foreign gene.[14] Furthermore, MPV replication in non-human primates (NHPs) was highly restricted, presumably due to a strong host-range restriction,[13,14] but MPV vectors expressing RSV F still induced strong serum RSV-neutralizing antibody responses that were comparable to those induced by wild-type RSV.[14] These features along with its tropism for epithelial cells in the respiratory tract identify MPV as an attractive candidate for mucosal vaccination via the respiratory route. The live-attenuated MPV vector vaccine candidates of the present study were designed for intranasal immunization to directly induce mucosal immunity to SARS-CoV-2 in the respiratory tract, in addition to stimulating systemic immunity.

Most of the current injectable COVID-19 vaccines are based on prefusion-stabilized versions of the SARS-CoV-2 S protein, the major neutralization and protective antigen of SARS-CoV-2.[15,16] Prefusion-stabilization by introduction of proline substitutions prevents this antigen

[1]RNA Viruses Section, Laboratory of Infectious Diseases, National Institute of Allergy and Infectious Diseases, National Institutes of Health, Bethesda, MD 20892, USA
[2]Experimental Primate Virology Section, Comparative Medicine Branch, National Institute of Allergy and Infectious Diseases, National Institutes of Health, Poolesville, MD 20837, USA
[3]Research Technologies Branch, Rocky Mountain Laboratories, National Institute of Allergy and Infectious Diseases, National Institutes of Health, Hamilton, MT 59840, USA
[4]SARS-CoV-2 Virology Core, Laboratory of Viral Diseases, National Institute of Allergy and Infectious Diseases, National Institutes of Health, Bethesda, MD 20892, USA
[5]Lead contact
*Correspondence: ubuchholz@niaid.nih.gov
https://doi.org/10.1016/j.isci.2023.108490

from forming a post-fusion conformation and keeps the protective epitopes of the receptor binding domain (RBD) exposed. Indeed, in previous studies, the prefusion-stabilized versions of S were shown to be more physically stable and immunogenic than wild-type S.[17,18]

In the present report, we constructed MPV vectors expressing the native or prefusion-stabilized version of the SARS-CoV-2 S protein, performed *in vitro* comparisons, and evaluated the two vectors for safety and immunogenicity in rhesus macaques.

RESULTS

Generation of MPV/S and MPV/S-2P and characterization in cell culture

We previously generated an MPV vaccine vector based on a recombinant version of MPV strain 15.[14] Because of concerns of possible over-attenuation due to the addition of a supernumerary gene into the MPV vector, we partially codon-pair optimized the L open reading frame (ORF) encoding the MPV polymerase[14]. To generate a version of MPV expressing the SARS-CoV-2 S protein, the ORF encoding the S protein (aa 1-1,273) of the ancestral SARS-CoV-2 S protein (GenBank MN908947) was codon-optimized for expression in humans. A second version of this optimized S ORF incorporated two proline substitutions ([K986P] and [V987P]), which stabilized S in the prefusion conformation, and the S1/S2 furin cleavage site was ablated (S-2P[16]) (Figure 1A), rendering the S protein non-functional for virus entry. To generate MPV/S and MPV/S-2P, the S and S-2P ORFs were placed under control of MPV transcription signals and inserted, using cDNAs of the MPV antigenome (a positive-sense copy of the genome), at the third genome position in the MPV genome, between the MPV nonstructural protein 2 (NS2) and nucleoprotein (N) genes (Figure 1A). This genome position had previously been determined to provide strong and stable expression of foreign genes.[14] MPV/S and MPV/S-2P as well as the empty-vector control MPV were readily rescued by reverse genetics and amplified in Vero cells. Virus stocks were prepared and whole-genome sequencing of each stock confirmed the absence of adventitious mutations. We evaluated the stability of S expression by titration and dual-staining immunoplaque assays of each virus stock using a rabbit hyperimmune serum against MPV ([14], immunostaining visualized in red) and a monoclonal antibody targeting the S protein (CR3022, visualized in green), revealing that 100% of the MPV/S and MPV/S-2P plaques expressed S (Figure 1B, yellow).

We evaluated multicycle replication of the MPV vectors in Vero cells, which are a suitable substrate for vaccine manufacture and lack a functional type 1 IFN response, and A549 cells, which represent human airway epithelial cells (Figures 1C and 1D). Following infection at a multiplicity of infection (MOI) of 0.1, MPV/S and MPV/S-2P replicated similarly to MPV in both cell lines (Figure 1C), indicating that the presence of the additional gene did not affect replication. All viruses replicated to high titers in Vero cells, while replication in A549 cells was much less efficient. In both cell lines, S or S-2P expression remained stable over 10 days of replication (Figure 1D).

To characterize viral protein expression, we infected Vero and A549 cells with MPV, MPV/S, or MPV/S-2P at an MOI of 2 (2 independent experiments, with duplicate wells in each experiment). Fifty-six hours after infection, we prepared cell lysates for analysis of viral protein expression by SDS-PAGE under denaturing and reducing conditions, followed by western blotting. Quantitative imaging of infrared immunostaining showed that the S protein had accumulated to about 1.1- to 1.6-fold higher levels in MPV/S-2P-infected Vero cells than in MPV/S infected Vero cells (Figure 2A, left and right panels). Smaller bands consistent with cleaved S1 and S2 subunits were present in MPV/S-infected cells, but not in MPV/S-2P infected cells, confirming the absence of proteolytic cleavage of S-2P. No difference in the accumulation of the MPV nucleoprotein N was detected between MPV, MPV/S, and MPV/S-2P infected Vero cells over time, but a 3-fold decrease in expression of the MPV phosphoprotein P in MPV/S-infected cells compared to MPV- and MPV/S-2P infected cells, respectively, was noted. Finally, we detected a significant 4-fold lower level of expression of the MPV attachment protein G in MPV/S- and MV/S-2P-infected Vero cells compared to MPV-infected cells (Figure 2A), suggesting that S glycoprotein expression might be associated with a reduction in expression or processing of the heavily glycosylated MPV attachment protein G.

We also evaluated the protein content of purified virus particles (Figure 2B). Aliquots from each virus stock were purified by ultracentrifugation through 30%/60% sucrose cushions, followed by SDS-PAGE and western blotting or silver staining (Figure 2B). No protein band consistent with S was detectable in purified MPV or MPV/S preparations, but we identified a strong band consistent with S0 protein in purified MPV/S-2P particles, suggesting that the S protein was associated with MPV/S-2P, but not with MPV/S virus particles. No apparent differences in MPV N and P content were detected between the purified virus preparations, but we detected weaker bands of MPV G in MPV/S-2P and MVP/S preparations compared to the MPV control by western blot. Electron microscopy of purified MPV/S-2P and MPV particles showed that MPV formed long viral filaments typical of pneumoviruses. Since we had detected S0 specific signals by western blot in purified MPV/S-2P, we further evaluated MPV/S-2P particles by immunogold labeling to confirm that the S protein was associated with virions. Indeed, S-specific immunogold labeling was abundant on the MPV/S-2P virions, but not on MPV particles, confirming the presence of S on the MPV/S-2P particles (Figure 2C).

MPV and derivatives replicate to low levels and are safe in macaques

To compare the replication, safety, and immunogenicity of the MPV/S and MPV/S-2P vaccine candidates, we immunized rhesus macaques (n = 4 per group) intranasally and intratracheally (IN/IT) with 6.3 $\log_{10}$ plaque-forming units (PFU) of MPV (empty vector control), MPV/S or MPV/S-2P (see Figure 3A for study design and sample collection). Nasopharyngeal swabs (NSs) and tracheal lavages (TLs) were collected over 15 days post-immunization (pi) to evaluate vaccine virus shedding in the upper airways (UAs) and lower airways (LAs).

We detected shedding of MPV and derivatives in the UA in all animals, but only sporadically and at low levels ($\leq 2 \log_{10}$ PFU/ml, Figure 3B, left panel). In the LA, shedding of MPV and derivatives was also low and sporadic, with MPV replicating the most efficiently (geometric mean peak titers [GMT] of 2.5 $\log_{10}$ PFU/ml on day 6 pi); MPV/S2-P was detectable in the LA of all animals, albeit one animal (#2) only had virus

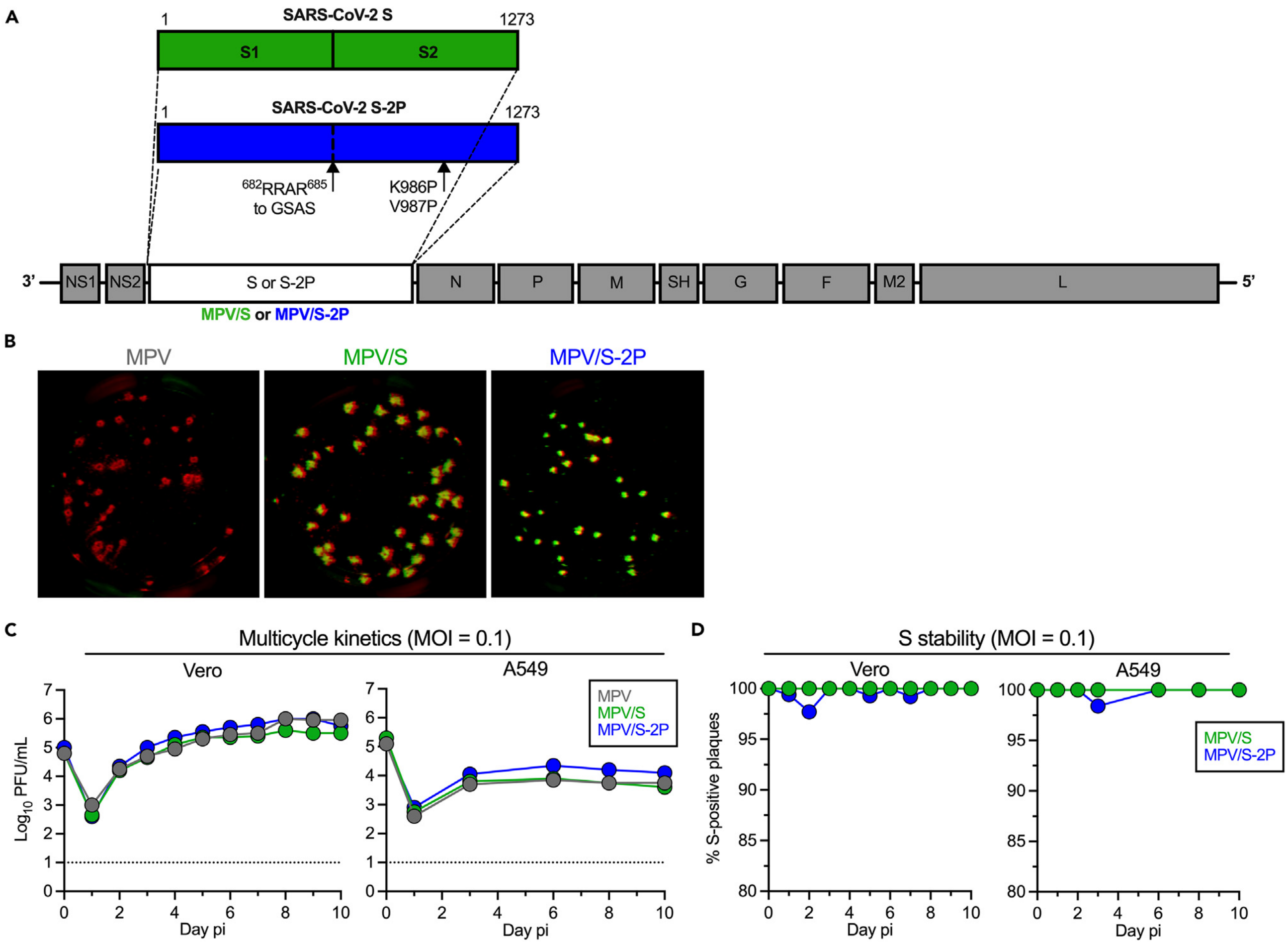

Figure 1. Genome organization of MPV and derivatives; characterization in cell culture

(A) Schematic representation of the MPV genome (gray) and two versions of the inserted SARS-CoV-2 S ORFs, namely S (green) and S-2P (blue) inserted between the NS2 and N genes. S is the full-length wild-type S ORF (aa 1-1,273) of the ancestral SARS-CoV-2 (Wuhan-1), codon-optimized for optimal expression in humans. The S1 and S2 subunits are indicated. S-2P is a version of the S ORF with two proline substitutions ([K986P] and [V987P]), introduced to stabilize S in the prefusion form, and with the furin cleavage site "RRAR" replaced by "GSAS" residues, indicated by arrows.[16] Reverse genetics was used to recover the MPV/S, MPV/S-2P, and empty MPV vector.

(B) Plaque phenotype in Vero cells. MPV proteins were detected using an MPV-specific rabbit hyperimmune serum, and SARS-CoV-2 S was detected using the human anti-S monoclonal antibody CR3022. Infrared fluorophore-labeled secondary antibodies were used to visualize MPV and S in red and green, respectively, with double-positive plaques appearing yellow.

(C) Multicycle growth kinetics *in vitro*. Duplicate monolayers of Vero and A549 cells were infected at an MOI of 0.1 with MPV, MPV/S, or MPV/S-2P and incubated at 32°C. At indicated time points, cells were scraped into the supernatants. Supernatants were clarified by centrifugation, and titers were determined by dual-staining immunoplaque assay. Mean titers, standard deviation (not visible due to low deviation) and limit of detection (dotted line; 10 plaque-forming units (PFU)/mL) are shown.

(D) Stability of S protein expression by MPV/S and MPV/S-2P, measured by dual-staining immunoplaque assay, and expressed as the percentage of S-positive plaques out of total plaques at the indicated time point.

detectable on a single day (day 6) at the level of detection. All macaques cleared MPV and derivatives from the UA and LA by day 8 and 12 post-immunization (pi), respectively. Thus, following IN/IT immunization, MPV replication was highly restricted in rhesus macaques, as shown previously.[13,14] No changes in vital signs were observed following immunization of macaques with MPV or derivatives (Figure S1), indicating that MPV is safe in macaques.

MPV/S-2P induced a stronger mucosal anti-S antibody response than MPV/S

Nasal wash (NW) was collected before immunization and on days 15, 21, and 28 after immunization to determine the mucosal antibody response (Figure 4). Despite its low level of replication, MPV/S-2P induced anti-S and anti-RBD IgG (Figure 4A) and IgA (Figure 4B) responses in the UA of all four animals. GMTs of anti-S and anti-RBD IgG and IgA in MPV/S-2P-immunized animals peaked at 21 days pi (Figures 4A and 4B). Compared to

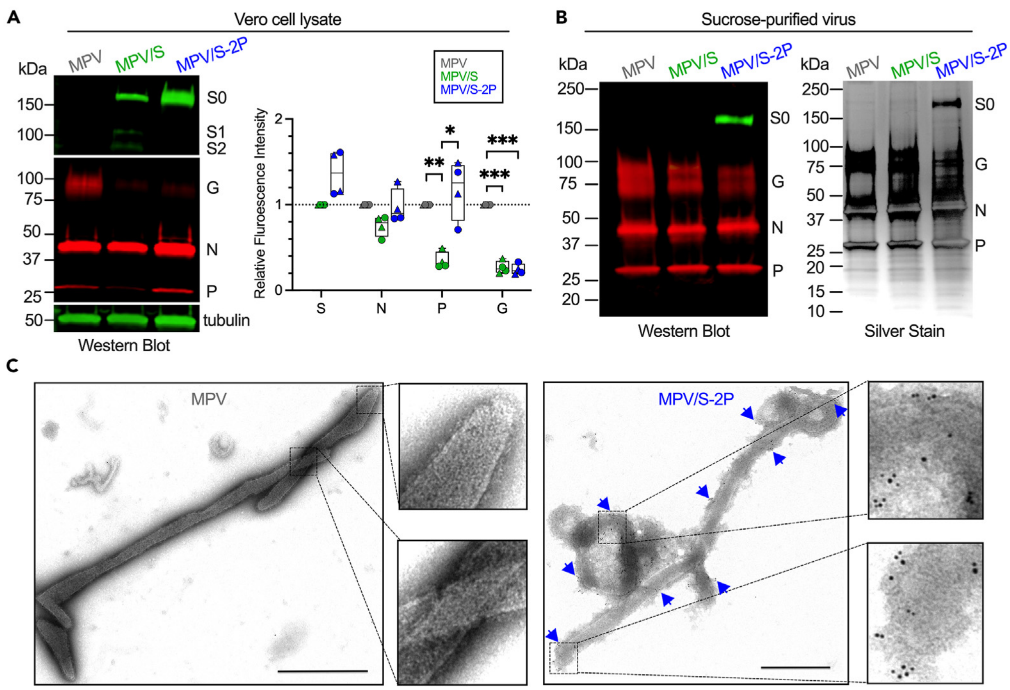

Figure 2. Viral proteins in lysates of infected Vero cells and purified virus particles

(A) Viral protein expression in lysates of infected Vero cells. Vero cell monolayers were infected at an MOI of 2 PFU/cell with MPV or derivatives. After incubation at 32°C for 56 h, cell lysates were prepared, subjected to SDS-PAGE under denaturing and reducing conditions, and analyzed by western blot using a rabbit anti-MPV hyperimmune serum that detects MPV G, N, and P proteins, and a goat anti-S-2P hyperimmune serum that detects the uncleaved form of S as well as S1 and S2 subunits.[18] A mouse anti-tubulin monoclonal antibody was used to detect tubulin, serving as a loading control. Blots were further incubated with infrared fluorophore-labeled secondary antibodies. Infrared fluorescence was scanned using an Odyssey CLX, analyzed using Image Studio software, normalized to tubulin, and expressed as relative fluorescence intensity compared to MPV (N, P, G proteins) or MPV/S (S protein). Representative blots with protein bands indicated are shown in the left panel, and data from n = 4 different wells from 2 independent experiments (with wells from the same experiment represented by the same symbol) are shown in the right panel. Individual values and medians are shown (*$p < 0.05$, **$p < 0.005$, ***$p < 0.001$; two-way ANOVA for N, P, and G proteins with Tukey post-test).

(B) Sucrose-purified virions (1 μg/lane) were analyzed by western blotting (as described under A) and silver staining. Molecular weight markers are indicated on the left, and the identities of the protein bands are shown on the right.

(C) Electron micrographs with S-specific immunogold labeling of MPV and MPV/S-2P particles to confirm the incorporation of S protein into MPV/S2-P particles. Sucrose-purified MPV and MPV/S-2P virus stocks were incubated with goat anti-S serum and immunogold-labeled secondary antibody. Representative images of filamentous MPV and MPV/S-2P particles are shown with scale bars indicating 500 nm. The blue arrows indicate clusters of gold beads associated with MPV/S-2P particles, indicative of the presence of S, with two areas enlarged for visualization.

MPV/S-2P, mucosal antibody responses induced by MPV/S were more variable and lower ($p = 0.0047$ and $p = 0.0013$ for anti-RBD IgG and IgA at day 21). As expected, no anti-S mucosal antibodies were detected in animals immunized with the MPV control (Figures 4A and 4B).

Mucosal immunization with MPV/S-2P induced high serum anti-S antibody titers

IN/IT immunization also induced high levels of serum anti-S and anti-RBD IgG and IgA as early as day 15 pi (Figures 5A and 5B). The serum IgG titers to S and RBD in MPV/S-2P immunized animals (GMTs of 4.8 and 5.5 $\log_{10}$, respectively, detected on day 28 pi; Figure 5A) were 5- and 32-fold higher, respectively, than those in plasma from 23 SARS-CoV-2 convalescent human donors (Figure 5A, red symbols). Serum antibodies from three MPV/S- and two MPV/S-2P-immunized macaques neutralized the vaccine-matched WA1/2020 strain, but the neutralizing activity was relatively low (Figure 5C, left panel). As expected, no anti-S serum antibodies were induced by the empty vector control (Figure 5). MPV and derivatives also induced strong serum neutralizing antibodies against the MPV vector itself (Figure 5C, right panel).

As a surrogate to additional BSL-3 neutralization assays, we evaluated the ability of serum antibodies to inhibit binding of soluble ACE2 receptor to purified S proteins of SARS-CoV-2 variants. We incubated serum samples on plates coated with purified S proteins from 18 SARS-CoV-2 variants and determined the percentage of ACE2 binding inhibition by serum antibodies (Figures 5 and S2). The strongest ACE2 binding inhibition by serum antibodies was detected for the vaccine-matched S protein derived from strain WA1/2020, with peak median inhibition rates of 94% and 97% for sera from MPV/S and MPV/S-2P immunized animals, respectively, on day 21 post-immunization (Figure 5D). We

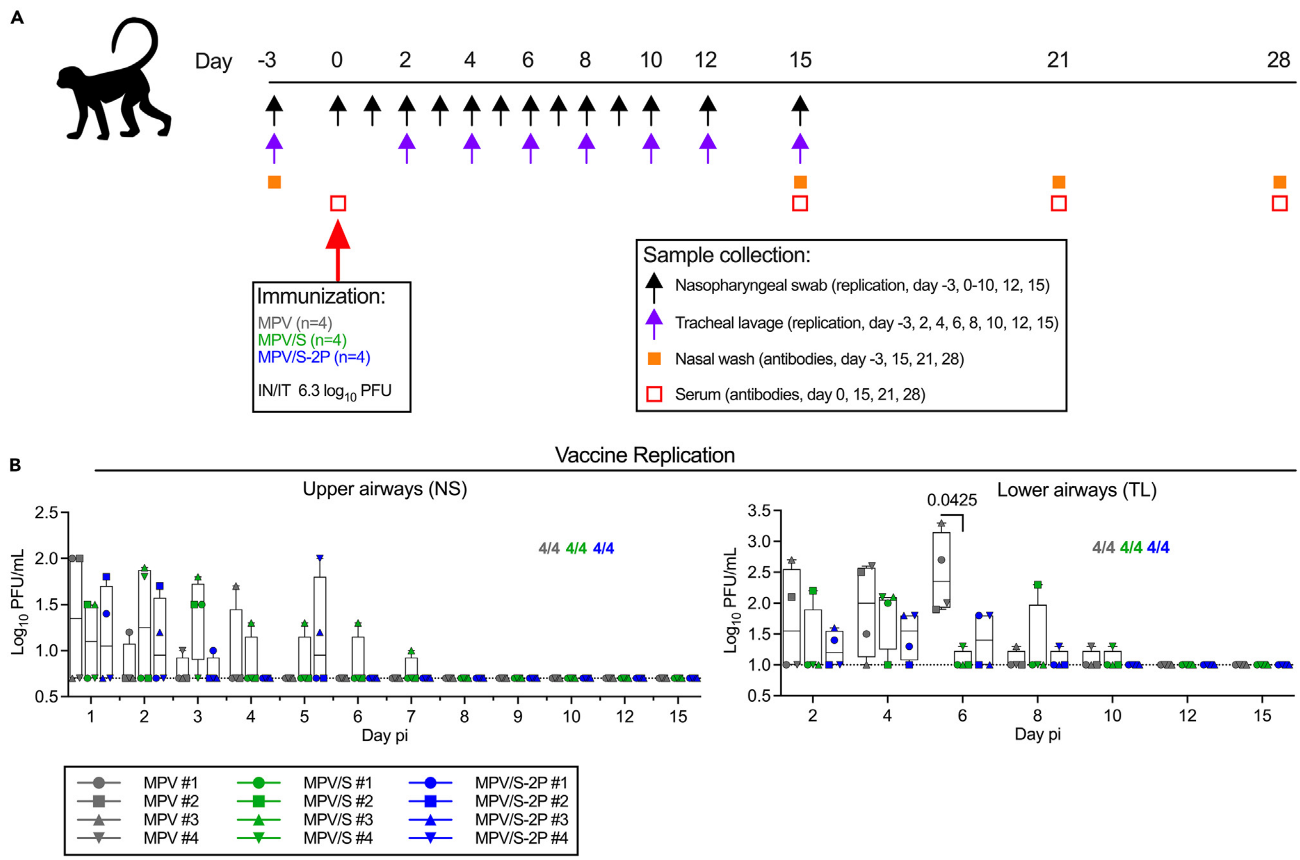

Figure 3. Replication of MPV and derivatives in rhesus macaques

(A) Timeline of the macaque study to evaluate safety, replication, and immunogenicity of MPV/S and MPV/S-2P. Three groups of four macaques each were immunized by the IN/IT route with 6.3 $\log_{10}$ PFU of MPV, MPV/S, and MPV/S-2P. Macaques were monitored daily (Figure S1) and nasopharyngeal swab (NS), tracheal lavage (TL), nasal wash (NW), and serum were collected at the indicated day post-immunization (pi).

(B) Replication of MPV and derivatives in the upper and lower airways of macaques. Vaccine titers were evaluated by plaque assay on Vero cells from NS and TL collected at the indicated day pi and expressed in $\log_{10}$ PFU/ml. The limits of detection (0.7 $\log_{10}$ for NS; 1 $\log_{10}$ for TL) are indicated by a dotted line. The medians, min and max values, 25th and 75th quartiles, and individual values are shown, with each animal represented by a different symbol. The p value for the significant difference in TL results on day 6 is indicated (two-way ANOVA with Tukey post-test; $p < 0.05$). The number of macaques in each group with replicating virus is indicated in each graph.

See also Figure S1.

also detected serum ACE2 binding inhibition against S proteins of the alpha, beta, delta, and French variants with median inhibition rates on day 21 ranging from 43% to 83% for MPV/S and 62% to 92% for MPV/S-2P (Figures 5D and S2). We also evaluated ACE2 binding inhibition for S proteins from 13 different Omicron variants. The inhibition rates were low, with medians ranging from 0% to 23% for sera collected on day 21 following immunization with MPV/S or MPV/S-2P, only slightly higher than the background in empty-vector control immunized animals (median 0% to 16%) (Figures 5D and S2). Overall, these results confirmed that MPV/S-2P expressing the prefusion-stabilized S-2P antigen was more immunogenic than MPV/S expressing the native S protein.

DISCUSSION

In the present study, we used the non-human virus MPV as a live-attenuated viral vector for mucosal delivery to the respiratory tract, designed to express a prefusion-stabilized version of SARS-CoV-2 S, and evaluated its safety and immunogenicity in rhesus macaques. In previous NHP studies, MPV was highly immunogenic, yet strongly attenuated following administration by the IN/IT route. Even though these vector vaccine candidates will be delivered intranasally by nasal sprayer in future clinical studies, we chose for this study the IN/IT route because it reduces animal-to-animal variability in vaccine "take", and is expected to provide for the most stringent evaluation of vaccine safety in NHPs.

Pneumoviruses typically are restricted in their replication to the superficial epithelial cells of the respiratory tract, and not likely to spread and replicate in non-respiratory tissues, increasing the safety of MPV as a vector. The attenuation of MPV in primates relies on host range restriction; a strong host range restriction typically resides in multiple genes and is refractory to de-attenuation.[21,22] Another important factor

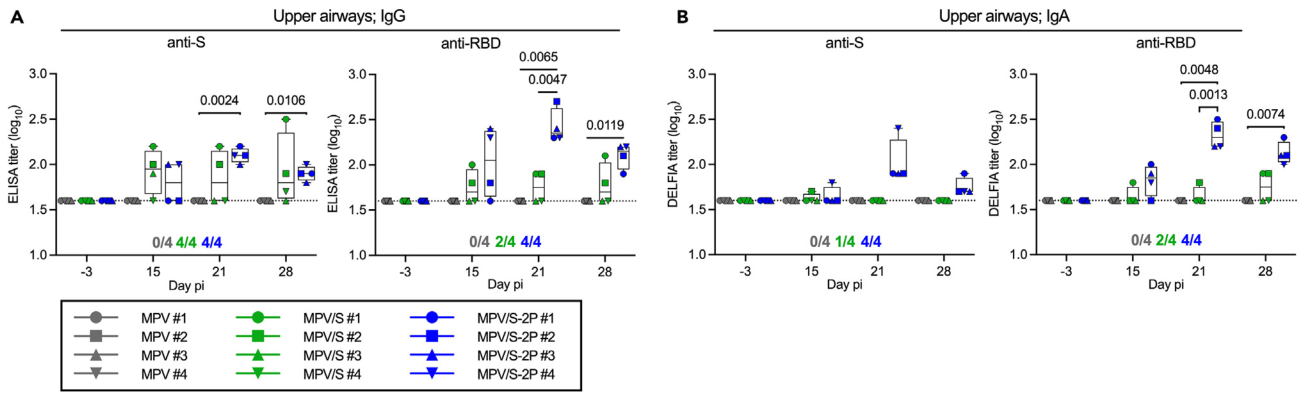

Figure 4. MPV/S-2P induces stronger mucosal anti-S antibody response than MPV/S

Nasal wash samples (NW) were collected on the indicated day pi, and the levels of mucosal IgG (A) and IgA (B) specific to SARS-CoV-2 S protein (A and B, left panels) or its receptor binding domain (RBD; A and B, right panels) in NW were determined using an immunoassay that measures IgG and IgA in sequential reads (see STAR Methods). Plates were coated with SARS-CoV-2 S protein (left panels) or RBD (right panels), and incubated with serially diluted NW. (A) Bound IgG was detected by ELISA using a horseradish peroxidase (HRP) conjugated secondary antibody and an HRP electrochemiluminescence substrate (first read). (B) Subsequently, bound IgA on each plate was detected using a biotinylated secondary antibody to the IgA alpha chain in a streptavidin-Europium based dissociation-enhanced lanthanide fluorescence assay (DELFIA; second read). While the IgA specific secondary antibody does not discern between monomeric or polymeric or secretory isoforms, in mucosal secretions, about 80% of total IgA typically is polymeric or secretory IgA derived from mucosal IgA-secreting B cells.[19,20] The limit of detection (1.6 log_{10}) is indicated by a dotted line. The medians, min and max values, 25th and 75th quartiles, and individual values are shown, with each animal represented by a different symbol. Adjusted p values are indicated ($p < 0.05$, two-way ANOVA with Tukey post-test). The number of macaques in each group with detectable mucosal antibodies is indicated in each graph.

in our choice of MPV as a vector was the general absence of pre-existing immunity to MPV in humans, obviating concerns of immune restriction of the immunizing vector.

Similarly to previous studies that evaluated MPV or an MPV-based vector in NHPs,[13,14] replication of MPV, MPV/S, and MPV/S-2P in the UA of macaques was very low and sporadic, peaking at approximately 2 log_{10} PFU/ml. These results predict that MPV vectors will be highly attenuated and restricted in replication and shedding in humans. Previous experience in humans with attenuated strains of influenza, human parainfluenza (HPIV) and RSVs as vaccines or vaccine candidates has shown that intranasal administration of an attenuated respiratory virus typically results in reduced infection and replication compared to the wild-type virus; in case of an attenuated virus, infection typically requires a higher-titer inoculum, and virus shedding is low and reduced in duration. The possibility of transmission is greatly reduced because a low titer of shed attenuated virus typically is inefficient at initiating infection and replication. For example, the transmissibility of the live-attenuated influenza virus vaccine FluMist was studied in a child-care setting.[23] The study included 98 vaccine recipients, with a single incident of confirmed transmission to a single placebo recipient. FluMist titers recovered in nasal secretions of pediatric vaccinees typically are in the range of up to 4 log_{10} per mL, orders of magnitudes higher than those expected for MPV/S-2P. Transmissibility of another live-attenuated intranasal pediatric vaccine candidate, HPIV3 rcp45, also was evaluated in a child-care setting.[24] Following immunization, HPIV3 rcp45 shedding was detectable in 21 of 24 vaccinees, with a median duration of shedding of 14 days and median peak titers in nasal washes of 3.4 log_{10} PFU/mL. In this study, definite transmission was not detected in 26 placebo children, close contacts that were susceptible to HPIV3 infection and exposed to infected vaccinees in playgroups or household settings on a daily basis.[24] Since the infectivity and replication of MPV is orders of magnitude lower than for these influenza and HPIV3 examples, its transmissibility should be much lower. It also should be noted that MPV has been known for almost 85 years, and appears to be widespread globally, but there have not been any reports of direct detection of MPV in humans, whether by classic virologic methods or, in recent years, by molecular diagnostics through widespread use of high-throughput sequencing. Initial reports of MPV-specific antibodies in humans likely involved natural antibodies that had not been induced by infection.[13] These observations predict that transmission of MPV in humans would be highly inefficient, highly restricted, and non-pathogenic.

Regarding the risk of transmission to other animals, this potentially would involve mainly rodents. In the past, serological evidence of MPV infection was frequent in rodent colonies. The pathogenicity of MPV for inbred laboratory strains of mice varies substantially between mouse strains.[25] Due to infection control and surveillance measures, MPV now has been largely eliminated from laboratory animal colonies,[26–28] but outside of laboratory colonies, serological evidence of MPV can still be detected in rodents.[29] Natural MPV infections in rodents are subclinical and recognized mainly by serological evidence;[30] despite the widespread presence of MPV in nature, morbidity, or mortality attributable to natural MPV infections in wild or outbred mice has not been documented.[31,32] Overall, MPV is thought to be less readily transmitted in rodents than Sendai virus,[30] another respiratory pathogen of mice that is being developed as a vaccine vector.[33]

We readily recovered MPV/S and MPV/S-2P vaccine candidates expressing the wt S and the prefusion-stabilized S-2P, respectively. The preparation of vaccine material based on MPV is straight-forward because the vector remains fully replication-competent. Delivery is topical. Importantly for vaccine efficacy and manufacture, S expression by both MPV vectors remained stable over 10 days in cell culture, meaning that approximately 100% of viral infectious units retained expression of the S protein. S expression by the MPV vector was associated with reduced

CellPress
OPEN ACCESS

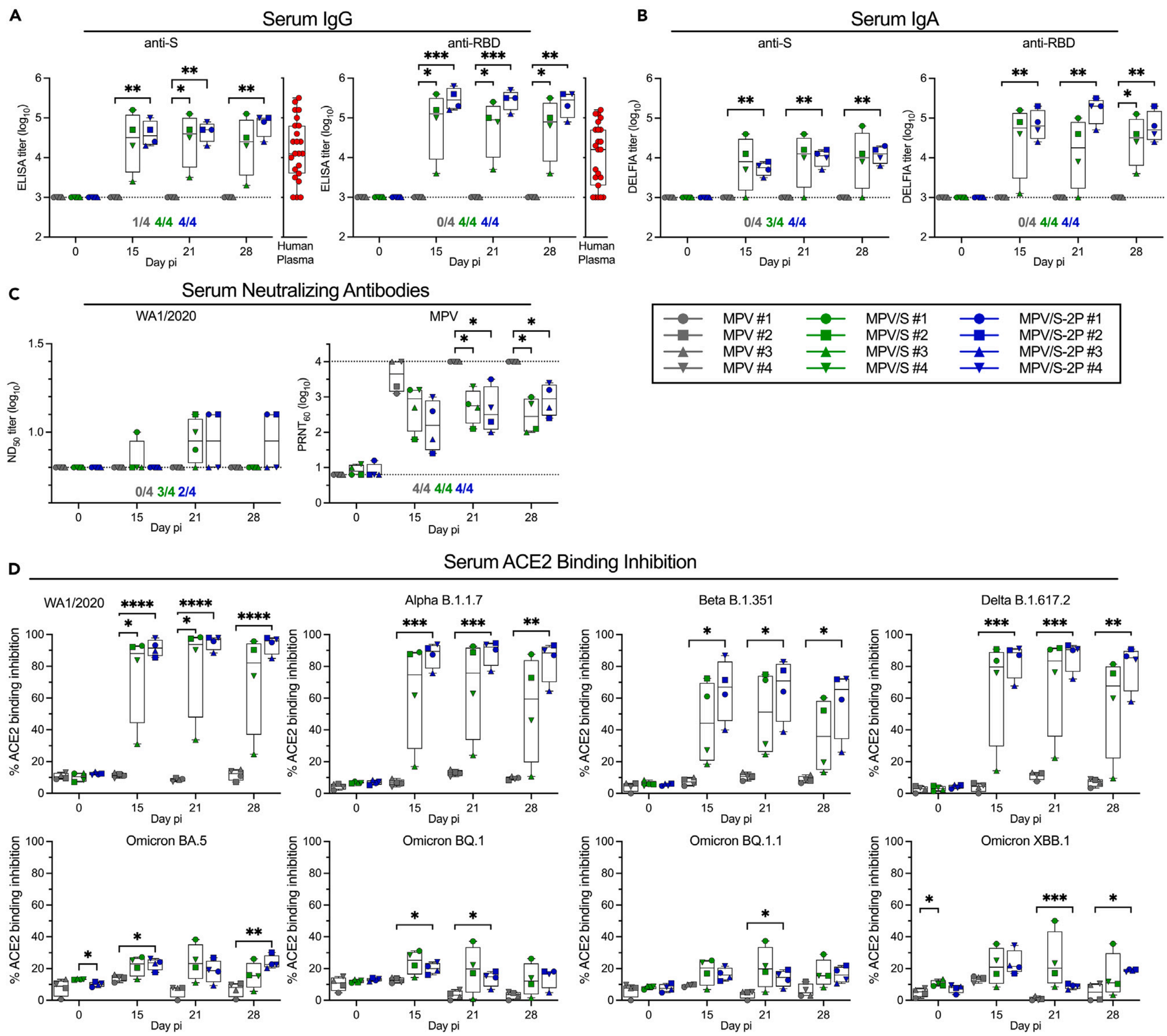

Figure 5. MPV/S-2P induced stronger systemic anti-S antibody response than MPV/S

Rhesus sera were collected on the indicated day pi, and the levels of serum IgG (A) and IgA (B) specific to SARS-CoV-2 S protein (A and B, left panels) or its receptor binding domain (RBD, A and B, right panels) were determined using an immunoassay that measures IgG (A) and IgA (B) in sequential reads (see STAR Methods). Plates were coated with SARS-CoV-2 S protein (A, B; left panels) or RBD (A, B; right panels), and incubated with serially diluted serum samples. (A) Bound serum IgG was detected by ELISA using a horseradish peroxidase (HRP) conjugated secondary antibody and an HRP electrochemiluminescence substrate (first read).

(B) Subsequently, bound serum IgA was detected using a biotinylated secondary antibody to the IgA alpha chain in a streptavidin-Europium based dissociation-enhanced lanthanide fluorescence assay (DELFIA; second read). While the IgA specific secondary antibody does not discern between monomeric or polymeric isoforms, serum IgA is primarily monomeric and originates from bone marrow.[19,20] Levels of anti-S and anti-RBD IgG antibodies in the plasma of 23 SARS-CoV-2 convalescent individuals (red) were determined for comparison. The limit of detection (3 log_{10}) is indicated by a dotted line.

(C) Serum neutralizing antibodies. The serum 50% neutralization titer (ND_{50}) against the vaccine-match SARS-CoV-2 WA1/2020 strain and the 60% plaque reduction neutralization titer ($PRNT_{60}$) against the vaccine vector MPV were determined. (A–C) The lower limit of detection is 0.8 log_{10} ND_{50} or $PRNT_{60}$, while the upper limit of detection for MPV neutralizing antibodies is 4.01 log_{10} $PRNT_{60}$. (A–C) The number of macaques in each group with detectable binding or neutralizing serum antibodies is indicated.

(D) Inhibition of binding of soluble, tagged ACE2 to the indicated purified S proteins by sera collected at the indicated day pi. Inhibition of ACE2 binding is expressed as % inhibition relative to a no-serum control. Binding inhibition to S proteins from other VoCs is shown in Figure S2. (A–D) The medians, min and max values, 25^{th} and 75^{th} quartile, and individual value are shown, with each animal represented by a different symbol. *$p < 0.05$, **$p < 0.01$, ***$p < 0.005$, ****$p < 0.0001$; two-way ANOVA with Tukey post-test.

See also Figure S2.

expression of the MPV attachment glycoprotein G but there were no apparent effects on viral replication *in vitro*. The lack of restriction due to the insert presumably accounts for its genetic stability, since there would be little selective advantage for mutations silencing expression. Creating further versions of this vaccine expressing S protein from other SARS-CoV-2 variants would be simple and rapid.

In cell culture, expression of S-2P by the MPV vector was higher than wt S, and S-2P was associated with the MPV virus particles. In other studies using a different negative-sense RNA virus vector for pediatric immunization, namely a live-attenuated chimeric bovine/human parainfluenza type-3 (B/HPIV3) vector,[18] we similarly found that prefusion-stabilization of SARS-CoV-2 S protein was associated with increased expression by the viral vector as well as increased incorporation in vector particles, suggesting that expression and incorporation of S into the envelopes of viral vectors may be facilitated by its stable conformation. Stabilization of the S protein in prefusion form has previously been shown to increase the induction of virus-neutralizing antibodies.[16,18] For another viral antigen, namely the RSV fusion glycoprotein F, we showed that incorporation of RSV F into the envelope of PIV1 and PIV3 vectors increases the response of virus-neutralizing antibody titers following intranasal immunization.[34–36] Several factors may contribute to the increased immunogenicity of antigen packaged into virions compared to strictly cell-associated antigen, including presentation in an ordered concentrated array, improved uptake of particles, improved uptake due to being in infectious virions, more rapid release compared to necrosis, and increased physical stability.[37]

A single IN/IT immunization of macaques with MPV/S-2P induced robust levels of mucosal anti-S and anti-RBD IgA and IgG, as well as serum anti-S and anti-RBD IgG. In serum, peak IgA and IgG titers ranged between 4 and 5 $\log_{10}$, while those in nasal washes did not exceed 3 $\log_{10}$. Using a classic neutralization assay to determine the 50% neutralization dose (ND_{50}) titer, we also detected SARS-CoV-2 virus neutralizing antibodies in serum but given the low sensitivity and dynamic range of this assay, we did not evaluate nasal wash specimens in an ND_{50} assay. Instead, we tried the more sensitive ACE2 binding inhibition assay. This assay serves as a surrogate for SARS-CoV-2 neutralization assays and measures the ability of antibodies in a sample to inhibit binding of soluble ACE2 receptor to purified S proteins of SARS-CoV-2 variants. However, while we were able to reproducibly detect ACE2 binding inhibiting antibodies in serum samples, we were unable to reliably detect binding inhibiting antibodies in samples from the UA (not shown), suggesting that nasal wash specimens are too dilute to detect antibodies in functional assays.

In the present study, we evaluated anti-S and RBD IgG and IgA in serum and nasal wash specimens using an IgG/IgA immunoassay. The strength of this assay is that the IgG and IgA antibody levels are determined in the same assay by sequential readings. However, the detection of IgA in this immunoassay relied on a secondary antibody that does not discern between IgA subclasses, nor between monomeric IgA (the primary form of IgA present in serum) and polymeric or secretory IgA (the primary forms present in nasal secretions). That said, serum IgA is predominantly monomeric and originates from bone marrow, while in airway secretions, polymeric and secretory IgA are predominant, representing about 80% of total IgA present in secretions,[19,20] and resulting from active transcytosis of IgA generated by mucosal IgA-secreting B cells.[38]

Overall, MPV/S-2P seemed more suitable to advance to further studies than MPV/S. While only the difference in induction of mucosal anti-RBD IgA and IgG reached significance, the overall results suggested that MPV/S-2P induces slightly higher levels of SARS-CoV-2 S and RBD specific serum antibodies. Serum anti-S IgG and IgA titers induced by MPV/S-2P were comparable to or higher than levels measured in the plasma of COVID-19 convalescent individuals. Thus, MPV/S-2P is emerging as the candidate of choice for additional studies. Since MPV vectors are highly immunogenic albeit being highly restricted in replication, there is a possibility that the immunogenicity of MPV vectors does not strongly depend on replication of the vaccine vector. If anti-vector immunity is not a huge factor in restricting the immunogenicity of MPV vectors, a second dose of MPV/S-2P might further improve the magnitude and duration of the S-specific immune responses. In addition, it would be of interest to evaluate the efficacy against SARS-CoV-2 replication and shedding of the intranasal vaccine candidate MPV/S-2P in a heterologous prime/boost study that includes a licensed injectable vaccine. This will be evaluated in future studies.

Limitations of the study

Firstly, this is a proof-of-concept study with the MPV vector expressing an S antigen derived from the ancestral version of SARS-CoV-2. While we were able to show considerable breadth of antibody reactivity in an ACE2 binding inhibition assay that included S proteins from 18 different SARS-CoV-2 variants and sub-variants, the S antigen expressed by the MPV vector will need to be updated prior to advancement to a clinical study. Secondly, in a BSL3 neutralization assay relying on live SARS-CoV-2, serum virus-neutralizing antibody titers were variable among MPV/S-2P-immunized macaques, likely due to low MPV vector replication following intranasal immunization. Thirdly, due to the small size of the NHP study and unavailability of female animals at the time of study, it was not possible to evaluate the association of sex or gender with study results. In this study, we were not able to show pre-clinical efficacy of the MPV-vectored vaccine candidates by evaluating the protection of macaques against SARS-CoV-2 challenge. The results of the present study suggest that the mucosal immunity in particular peaks about 3 weeks after mucosal immunization; a second dose of vaccine may be useful to expand the magnitude, breadth, and duration of the immune response. A two-dose study would also evaluate if the MPV vector itself will be affected by the strong anti-vector immunity that we detected following a single dose.

STAR★METHODS

Detailed methods are provided in the online version of this paper and include the following:

- Materials availability
- Data and code availability
- EXPERIMENTAL MODEL AND SUBJECT DETAILS
  - Cell lines
  - SARS-CoV-2 virus stocks
  - Animals
- METHOD DETAILS
  - Generation of MPV and derivatives
  - Dual-staining immunoplaque assay
  - Multicycle kinetics of MPV and derivatives in cell culture
  - SDS-page and Western blotting
  - Sucrose purification of MPV virus stock and derivatives
  - Electron microscopy of sucrose-purified MPV preparations
  - Replication of MPV and derivatives in the upper and lower airways of macaques
  - Dual IgG and IgA assay to detect anti-S or anti-RBD antibodies
  - Serum neutralization assay of SARS-CoV-2 and MPV
  - ACE2 binding inhibition assays
- QUANTIFICATION AND STATISTICAL ANALYSIS
  - Statistics

SUPPLEMENTAL INFORMATION

Supplemental information can be found online at https://doi.org/10.1016/j.isci.2023.108490.

ACKNOWLEDGMENTS

We thank Jeffrey I. Cohen, Laboratory of Infectious Diseases, NIAID, NIH, for providing plasma from SARS-CoV-2 convalescent anonymized individuals, and Peter L. Collins for helpful discussions and comments on the manuscript. This research was supported by the Intramural Research Program of the NIAID, NIH (Project number ZIA AI001298-01).

AUTHOR CONTRIBUTIONS

Conceptualization: S.M. and U.J.B. design of experiments: J.A.K., X.L., C.L., Y.M., C.S., L.Y., R.H., A.C., D.W.D., E.R.F., H.S.P., C.L.N., and U.J.B. investigation: J.A.K., X.L., C.L., Y.M., C.S., L.Y., R.H., A.C., D.W.D., S.M., C.L.N., and U.J.B. reagent development: R.F.J., S.A., and S.M. data analysis and visualization: J.A.K., X.L., C.L., Y.M., C.S., L.Y., R.H., A.C., D.W.D., E.R.F., C.L.N., and U.J.B. writing – original draft: J.A.K., C.L.N., and U.J.B. writing – review and editing: J.A.K., X.L., C.L., Y.M., C.S., L.Y., R.H., A.C., D.W.D., E.R.F., R.F.J., H.S.P., S.A., S.M., C.L.N., and U.J.B.

DECLARATION OF INTERESTS

U.J.B., C.L.N., S.M., C.L., and J.K. are inventors on a provisional patent application entitled "Recombinant murine pneumonia virus expressing severe acute respiratory syndrome coronavirus 2 (SARS-CoV-2) spike protein", filed by the United States, Department of Health and Human Services.

INCLUSION AND DIVERSITY

We support inclusive, diverse, and equitable conduct of research.

Received: June 22, 2023
Revised: August 13, 2023
Accepted: November 14, 2023
Published: November 22, 2023

REFERENCES

1. Response, W.T.E. (2023). COVID-19 Weekly Epidemiological Update (World Health Organization). https://www.who.int/publications/m/item/weekly-epidemiological-update-on-covid-19—8-march-2023.
2. Wu, F., Zhao, S., Yu, B., Chen, Y.M., Wang, W., Song, Z.G., Hu, Y., Tao, Z.W., Tian, J.H., Pei, Y.Y., et al. (2020). A new coronavirus associated with human respiratory disease in China. Nature *579*, 265–269.
3. Argenziano, M.G., Bruce, S.L., Slater, C.L., Tiao, J.R., Baldwin, M.R., Barr, R.G., Chang, B.P., Chau, K.H., Choi, J.J., Gavin, N., et al. (2020). Characterization and clinical course of 1000 patients with coronavirus disease 2019 in New York: retrospective case series. BMJ *369*, m1996.
4. Suleyman, G., Fadel, R.A., Malette, K.M., Hammond, C., Abdulla, H., Entz, A., Demertzis, Z., Hanna, Z., Failla, A., Dagher, C., et al. (2020). Clinical Characteristics and Morbidity Associated With Coronavirus Disease 2019 in a Series of Patients in

Metropolitan Detroit. JAMA Netw. Open 3, e2012270.
5. Anderson, E.J., Rouphael, N.G., Widge, A.T., Jackson, L.A., Roberts, P.C., Makhene, M., Chappell, J.D., Denison, M.R., Stevens, L.J., Pruijssers, A.J., et al. (2020). Safety and Immunogenicity of SARS-CoV-2 mRNA-1273 Vaccine in Older Adults. N. Engl. J. Med. 383, 2427–2438.
6. Corbett, K.S., Edwards, D.K., Leist, S.R., Abiona, O.M., Boyoglu-Barnum, S., Gillespie, R.A., Himansu, S., Schäfer, A., Ziwawo, C.T., DiPiazza, A.T., et al. (2020). SARS-CoV-2 mRNA vaccine design enabled by prototype pathogen preparedness. Nature 586, 567–571.
7. Sadoff, J., Gray, G., Vandebosch, A., Cárdenas, V., Shukarev, G., Grinsztejn, B., Goepfert, P.A., Truyers, C., Fennema, H., Spiessens, B., et al. (2021). Safety and Efficacy of Single-Dose Ad26.COV2.S Vaccine against Covid-19. N. Engl. J. Med. 384, 2187–2201.
8. Walsh, E.E., Frenck, R.W., Jr., Falsey, A.R., Kitchin, N., Absalon, J., Gurtman, A., Lockhart, S., Neuzil, K., Mulligan, M.J., Bailey, R., et al. (2020). Safety and Immunogenicity of Two RNA-Based Covid-19 Vaccine Candidates. N. Engl. J. Med. 383, 2439–2450.
9. Mulligan, M.J., Lyke, K.E., Kitchin, N., Absalon, J., Gurtman, A., Lockhart, S., Neuzil, K., Raabe, V., Bailey, R., Swanson, K.A., et al. (2020). Phase I/II study of COVID-19 RNA vaccine BNT162b1 in adults. Nature 586, 589–593.
10. Fiolet, T., Kherabi, Y., MacDonald, C.J., Ghosn, J., and Peiffer-Smadja, N. (2022). Comparing COVID-19 vaccines for their characteristics, efficacy and effectiveness against SARS-CoV-2 and variants of concern: a narrative review. Clin. Microbiol. Infect. 28, 202–221.
11. Morens, D.M., Taubenberger, J.K., and Fauci, A.S. (2023). Rethinking next-generation vaccines for coronaviruses, influenzaviruses, and other respiratory viruses. Cell Host Microbe 31, 146–157.
12. Knisely, J.M., Buyon, L.E., Mandt, R., Farkas, R., Balasingam, S., Bok, K., Buchholz, U.J., D'Souza, M.P., Gordon, J.L., King, D.F.L., et al. (2023). Mucosal vaccines for SARS-CoV-2: scientific gaps and opportunities-workshop report. NPJ Vaccines 8, 53.
13. Brock, L.G., Karron, R.A., Krempl, C.D., Collins, P.L., and Buchholz, U.J. (2012). Evaluation of pneumonia virus of mice as a possible human pathogen. J. Virol. 86, 5829–5843.
14. Brock, L.G., Liu, X., Liang, B., Lingemann, M., Liu, X., Herbert, R., Hackenberg, A.D., Buchholz, U.J., Collins, P.L., and Munir, S. (2018). Murine Pneumonia Virus Expressing the Fusion Glycoprotein of Human Respiratory Syncytial Virus from an Added Gene Is Highly Attenuated and Immunogenic in Rhesus Macaques. J. Virol. 92, e00723-18.
15. Hsieh, C.L., Goldsmith, J.A., Schaub, J.M., DiVenere, A.M., Kuo, H.C., Javanmardi, K., Le, K.C., Wrapp, D., Lee, A.G., Liu, Y., et al. (2020). Structure-based design of prefusion-stabilized SARS-CoV-2 spikes. Science 369, 1501–1505.
16. Wrapp, D., Wang, N., Corbett, K.S., Goldsmith, J.A., Hsieh, C.L., Abiona, O., Graham, B.S., and McLellan, J.S. (2020). Cryo-EM structure of the 2019-nCoV spike in the prefusion conformation. Science 367, 1260–1263.
17. Bos, R., Rutten, L., van der Lubbe, J.E.M., Bakkers, M.J.G., Hardenberg, G., Wegmann, F., Zuijdgeest, D., de Wilde, A.H., Koornneef, A., Verwilligen, A., et al. (2020). Ad26 vector-based COVID-19 vaccine encoding a prefusion-stabilized SARS-CoV-2 Spike immunogen induces potent humoral and cellular immune responses. NPJ Vaccines 5, 91.
18. Liu, X., Luongo, C., Matsuoka, Y., Park, H.S., Santos, C., Yang, L., Moore, I.N., Afroz, S., Johnson, R.F., Lafont, B.A.P., et al. (2021). A single intranasal dose of a live-attenuated parainfluenza virus-vectored SARS-CoV-2 vaccine is protective in hamsters. Proc. Natl. Acad. Sci. USA 118, e2109744118.
19. Delacroix, D.L., Dive, C., Rambaud, J.C., and Vaerman, J.P. (1982). IgA subclasses in various secretions and in serum. Immunology 47, 383–385.
20. Woof, J.M., and Mestecky, J. (2015). Chapter 17 - Mucosal Immunoglobulins. In Mucosal Immunology, J. Mestecky, W. Strober, M.W. Russell, B.L. Kelsall, H. Cheroutre, and B.N. Lambrecht, eds. (Academic Press), pp. 287–324.
21. Skiadopoulos, M.H., Schmidt, A.C., Riggs, J.M., Surman, S.R., Elkins, W.R., St Claire, M., Collins, P.L., and Murphy, B.R. (2003). Determinants of the host range restriction of replication of bovine parainfluenza virus type 3 in rhesus monkeys are polygenic. J. Virol. 77, 1141–1148.
22. Schmidt, A.C., McAuliffe, J.M., Huang, A., Surman, S.R., Bailly, J.E., Elkins, W.R., Collins, P.L., Murphy, B.R., and Skiadopoulos, M.H. (2000). Bovine parainfluenza virus type 3 (BPIV3) fusion and hemagglutinin-neuraminidase glycoproteins make an important contribution to the restricted replication of BPIV3 in primates. J. Virol. 74, 8922–8929.
23. Vesikari, T., Karvonen, A., Korhonen, T., Edelman, K., Vainionpää, R., Salmi, A., Saville, M.K., Cho, I., Razmpour, A., Rappaport, R., et al. (2006). A randomized, double-blind study of the safety, transmissibility and phenotypic and genotypic stability of cold-adapted influenza virus vaccine. Pediatr. Infect. Dis. J. 25, 590–595.
24. Madhi, S.A., Cutland, C., Zhu, Y., Hackell, J.G., Newman, F., Blackburn, N., Murphy, B.R., Belshe, R.B., Karron, R.A., Deatly, A.M., et al. (2006). Transmissibility, infectivity and immunogenicity of a live human parainfluenza type 3 virus vaccine (HPIV3cp45) among susceptible infants and toddlers. Vaccine 24, 2432–2439.
25. Anh, D.B.T., Faisca, P., and Desmecht, D.J.M. (2006). Differential resistance/susceptibility patterns to pneumovirus infection among inbred mouse strains. Am. J. Physiol. Lung Cell Mol. Physiol. 291, L426–L435.
26. Pritchett-Corning, K.R., Cosentino, J., and Clifford, C.B. (2009). Contemporary prevalence of infectious agents in laboratory mice and rats. Lab. Anim. 43, 165–173.
27. Zenner, L., and Regnault, J.P. (2000). Ten-year long monitoring of laboratory mouse and rat colonies in French facilities: a retrospective study. Lab. Anim. 34, 76–83.
28. Schoondermark-van de Ven, E.M.E., Philipse-Bergmann, I.M.A., and van der Logt, J.T.M. (2006). Prevalence of naturally occurring viral infections, Mycoplasma pulmonis and Clostridium piliforme in laboratory rodents in Western Europe screened from 2000 to 2003. Lab. Anim. 40, 137–143.
29. Dammann, P., Hilken, G., Hueber, B., Köhl, W., Bappert, M.T., and Mähler, M. (2011). Infectious microorganisms in mice (Mus musculus) purchased from commercial pet shops in Germany. Lab. Anim. 45, 271–275.
30. Schoeb, T.R. (2000). Respiratory diseases of rodents. Vet. Clin. North Am. Exot. Anim. Pract. 3, 481–496. vii.
31. Becker, S.D., Bennett, M., Stewart, J.P., and Hurst, J.L. (2007). Serological survey of virus infection among wild house mice (Mus domesticus) in the UK. Lab. Anim. 41, 229–238.
32. Kashuba, C., Hsu, C., Krogstad, A., and Franklin, C. (2005). Small mammal virology. Vet. Clin. North Am. Exot. Anim. Pract. 8, 107–122.
33. Russell, C.J., and Hurwitz, J.L. (2021). Sendai Virus-Vectored Vaccines That Express Envelope Glycoproteins of Respiratory Viruses. Viruses 13, 1023.
34. Liu, X., Liang, B., Ngwuta, J., Liu, X., Surman, S., Lingemann, M., Kwong, P.D., Graham, B.S., Collins, P.L., and Munir, S. (2017). Attenuated Human Parainfluenza Virus Type 1 Expressing the Respiratory Syncytial Virus (RSV) Fusion (F) Glycoprotein from an Added Gene: Effects of Prefusion Stabilization and Packaging of RSV F. J. Virol. 91, e01101-17.
35. Liu, X., Liang, B., Liu, X., Amaro-Carambot, E., Surman, S., Kwong, P.D., Graham, B.S., Collins, P.L., and Munir, S. (2020). Human parainfluenza virus type 3 expressing the respiratory syncytial virus pre-fusion F protein modified for virion packaging yields protective intranasal vaccine candidates. PLoS One 15, e0228572.
36. Liang, B., Ngwuta, J.O., Surman, S., Kabatova, B., Liu, X., Lingemann, M., Liu, X., Yang, L., Herbert, R., Swerczek, J., et al. (2017). Improved Prefusion Stability, Optimized Codon Usage, and Augmented Virion Packaging Enhance the Immunogenicity of Respiratory Syncytial Virus Fusion Protein in a Vectored-Vaccine Candidate. J. Virol. 91, e00189-17.
37. Liang, B., Ngwuta, J.O., Herbert, R., Swerczek, J., Dorward, D.W., Amaro-Carambot, E., Mackow, N., Kabatova, B., Lingemann, M., Surman, S., et al. (2016). Packaging and Prefusion Stabilization Separately and Additively Increase the Quantity and Quality of Respiratory Syncytial Virus (RSV)-Neutralizing Antibodies Induced by an RSV Fusion Protein Expressed by a Parainfluenza Virus Vector. J. Virol. 90, 10022–10038.
38. Russell, M.W., Moldoveanu, Z., Ogra, P.L., and Mestecky, J. (2020). Mucosal Immunity in COVID-19: A Neglected but Critical Aspect of SARS-CoV-2 Infection. Front. Immunol. 11, 611337.
39. Krempl, C.D., Wnekowicz, A., Lamirande, E.W., Nayebagha, G., Collins, P.L., and Buchholz, U.J. (2007). Identification of a novel virulence factor in recombinant pneumonia virus of mice. J. Virol. 81, 9490–9501.
40. Buchholz, U.J., Finke, S., and Conzelmann, K.K. (1999). Generation of bovine respiratory syncytial virus (BRSV) from cDNA: BRSV NS2 is not essential for virus replication in tissue culture, and the human RSV leader region acts as a functional BRSV genome promoter. J. Virol. 73, 251–259.
41. Chu, H., Chan, J.F.W., Yuen, T.T.T., Shuai, H., Yuan, S., Wang, Y., Hu, B., Yip, C.C.Y., Tsang, J.O.L., Huang, X., et al. (2020). Comparative tropism, replication kinetics, and cell damage profiling of SARS-CoV-2 and SARS-CoV with implications for clinical manifestations, transmissibility, and laboratory studies of

COVID-19: an observational study. Lancet Microbe *1*, e14–e23.

42. Ren, X., Glende, J., Al-Falah, M., de Vries, V., Schwegmann-Wessels, C., Qu, X., Tan, L., Tschernig, T., Deng, H., Naim, H.Y., and Herrler, G. (2006). Analysis of ACE2 in polarized epithelial cells: surface expression and function as receptor for severe acute respiratory syndrome-associated coronavirus. J. Gen. Virol. *87*, 1691–1695.

43. Park, H.S., Matsuoka, Y., Luongo, C., Yang, L., Santos, C., Liu, X., Ahlers, L.R.H., Moore, I.N., Afroz, S., Johnson, R.F., et al. (2022). Intranasal immunization with avian paramyxovirus type 3 expressing SARS-CoV-2 spike protein protects hamsters against SARS-CoV-2. NPJ Vaccines *7*, 72.

44. Le Nouen, C., Nelson, C.E., Liu, X., Park, H.S., Matsuoka, Y., Luongo, C., Santos, C., Yang, L., Herbert, R., Castens, A., et al. (2022). Intranasal pediatric parainfluenza virus-vectored SARS-CoV-2 vaccine is protective in monkeys. Cell *185*, 4811–4825.e7.

STAR★METHODS

KEY RESOURCES TABLE

REAGENT or RESOURCE	SOURCE	IDENTIFIER
Antibodies		
Anti-monkey IgG(H+L)-HRP	Thermo Fisher	Cat #PA1-84631; RRID: AB_933605
Anti-monkey IgA (alpha chain)-biotin	Alpha Diagnostic International	Cat #70049
Goat anti-human IgG(H+L)-HRP	Invitrogen	Cat #31410; RRID: AB_228269
Rabbit hyperimmune serum against MPV virions	RNA Viruses Section, LID, NIAID	N/A
Rabbit hyperimmune serum against MVA expressing MPV G	Krempl et al.[39]	N/A
Goat hyperimmune serum against SARS-CoV-2 S-2P	Liu et al., [18]	N/A
Anti-rabbit IRDye 680RD IgG	Li-Cor	Cat #926-68073; RRID: AB_10954442
Anti-goat IRDye 800CW IgG	Li-Cor	Cat #926-32214; RRID: AB_621846
Anti-human IRDye 800CW IgG	Li-Cor	Cat #926-32232; RRID: AB_10806644
Anti-rabbit Alexa Fluor 647 IgG (H+L)	ThermoFisher	Cat #A21245; RRID: AB_2535813
Donkey anti-goat IgG (H&L) conjugated to 6 nm gold beads	Aurion	Cat # 806.333
Bacterial and virus strains		
SARS-CoV-2 USA-WA1/2020 isolate	Natalie Thornburg et al., CDC	GenBank MN985325; GISAID: EPI_ISL_404895
Chemicals, peptides, and recombinant proteins		
SARS-CoV-2 S-2P	Liu et al.[18]	N/A
SARS-CoV-2 S RBD	Liu et al.[18]	N/A
SARS-CoV-2 S-2P-Avi	This paper	Avi-tagged S-2P
SARS-CoV-2 S RBD-Avi-His	This paper	Avi-tagged RBD
Aurion acetylated BSA (BSA-c)	EMS	Cat #25557
Critical commercial assays		
DELFIA time resolved fluorescence immunoassay	Perkin Elmer	N/A
Streptavidin-Europium	Perkin Elmer	Cat #1244-360
DELFIA Enhancement Solution	Perkin Elmer	Cat #4001-0010
ECL Substrate	Thermo Fisher	Cat #32106
V-PLEX SARS-CoV-2 Panel 25 (ACE2)	MSD	Cat #K15586U
V-PLEX SARS-CoV-2 Panel 32 (ACE2)	MSD	Cat #K15671U
QuikChange Lightning Multi Site-directed mutagenesis kit	Agilent	Cat # 210514
QIAamp Viral RNA Mini Kit	Qiagen	Cat #52904
Pierce Silver Stain Kit	Thermo Fisher	Cat #24612
1-Step Ultra TMB-ELISA	Thermo Scientific	Cat # 34028
Experimental models: Cell lines		
BSR T7/5	Buchholz et al. [40]	N/A
A549	ATCC	Cat #CCL-185
Vero	ATCC	Cat #CCL-81
Vero E6	ATCC	Cat #CRL-1586

(Continued on next page)

Continued

REAGENT or RESOURCE	SOURCE	IDENTIFIER
Vero E6 expressing human TMPRSS2	Liu et al.[18]	N/A
Experimental models: Organisms/strains		
Rhesus macaques (*Macaca mulatta*)	This paper	Young adult animals, 4-7 years of age, male. Animal study protocol approved by NIAID ACUC
Human plasma from SARS-CoV-2 convalescent donors, de-identified	Dr. Jeffrey I. Cohen, NIAID, NIH	Exempt from IRB review
Recombinant DNA		
MPV	Krempl et al.[39]	N/A
MPV/S	This paper	N/A
MPV/S-2P	This paper	N/A
MPV N, P, M2-1, and L helper plasmids	Krempl et al.[39]	N/A
SARS-CoV-2 S	Liu et al.[18]	GenBank MN908947
SARS-CoV-2 S-2P	Wrapp et al.[16]	N/A
SARS-CoV-2 S-6P	Generated as described in[15]	N/A
SARS-CoV-2 S RBD	Wrapp et al.[16]	N/A
Software and algorithms		
FlowJo v10	BD	https://www.flowjo.com
Prism v9	GraphPad Software, LLC	https://www.graphpad.com/scientificsoftware/prism/
ImageStudioLite 5.2.5	Li-Cor	https://www.licor.com/bio/image-studio-lite/resources#isl5
BioTek Gen 5	BioTek	https://www.biotek.com/products/software-robotics-software/gen5-microplate-reader-and-imager-software/

RESOURCE AVAILABILITY

Lead contact

- Requests for resources, reagents and further information regarding this manuscript should be addressed and will be fulfilled by the lead contact, Ursula Buchholz (ubuchholz@niaid.nih.gov).

Materials availability

- Plasmids and viruses newly generated in this study are available under material transfer request upon request to the lead contact.

Data and code availability

- All data are included in the manuscript.
- Any additional information required to reanalyze the data reported in this paper is available from the lead contact upon request.

EXPERIMENTAL MODEL AND SUBJECT DETAILS

Cell lines

Baby hamster kidney cells expressing T7 RNA polymerase (BSR T7/5; [40]) were used to recover MPV and derivatives and were grown in Glasgow minimum essential medium (MEM) (Thermo Fisher Scientific) supplemented with 10% Fetal bovine serum (FBS), 2 mM L-glutamine (Thermo Fisher Scientific), and 2% MEM Amino Acids (Thermo Fisher Scientific). African green monkey kidney Vero (ATCC CCL-81) and Vero E6 (ATCC CRL-1586) cells were grown in OptiMEM (Thermo Fisher) supplemented with 5% FBS. Human lung epithelial A549 cells (ATCC CCL-185) were grown in F12-K medium (ATCC) supplemented with 10% FBS. Vero and A549 cells were used for the characterization of the MPV vaccine candidates. Vero E6 cells were used for SARS-CoV-2 neutralization assays and titrations, whereas SARS-CoV-2 virus stocks were expanded using Vero E6 cells that express high levels of ACE2[41,42] or Vero E6 cells that stably express human TMPRSS2.[18]

SARS-CoV-2 virus stocks

The SARS-CoV-2 USA-WA1/2020 challenge virus (lineage A; GenBank MN985325 and GISAID accession ID: EPI_ISL_404895; obtained from Natalie Thornburg, Sue Gerber, and Sue Tong, Centers for Disease Control and Prevention [CDC], Atlanta, GA) was passaged twice on Vero E6 cells. The USA/CA_CDC_5574/2020 isolate (lineage B.1.1.7, GISAID: EPI_ISL_751801; sequence deposited by the CDC; isolate obtained from the CDC) and the USA/MD-HP01542/2021 isolate (lineage B.1.351, GISAID: EPI_ISL_890360; sequence deposited by Christopher Paul Morris, Chun Huai Luo, Adannaya Amadi, Matthew Schwartz, Nicholas Gallagher, and Heba H. Mostafa, The Johns Hopkins University; isolate obtained from Andrew Pekosz, The Johns Hopkins University, Baltimore, MD) were passaged on Vero E6 cells stably expressing TMPRSS2. Titration of SARS-CoV-2 stocks was performed by determination of 50% of the tissue culture infectious dose ($TCID_{50}$) in Vero E6 cells. All experiments with SARS-CoV-2 were conducted in Biosafety Level-3 containment laboratories approved for use by the US Department of Agriculture and CDC.

Animals

This animal study was approved by the NIAID Animal Care and Use Committee. Twelve juvenile and young adult male Indian-origin rhesus macaques (*Macaca mulatta*) were confirmed by SARS-CoV-2 S ELISA to be seronegative for SARS-CoV-2 prior to immunization. Animals were also confirmed to be negative for MPV neutralizing serum antibodies prior to immunization. Three groups of four macaques each were immunized intranasally (0.5 ml per nostril) and intratracheally (1 ml) with a total dose of 6.3 $\log_{10}$ PFU of MPV empty vector, MPV/S, or MPV/S-2P. Animals were monitored daily from day -3 through the end of the study. Each time they were sedated, macaques were checked for weight, rectal temperature, heart rate, respiratory rate, and blood oxygen levels.

The timelines and sampling schedules are diagrammed in Figure 3A. Nasopharyngeal swabs (NS) were performed on days -3, 0 to 10, 12, and 15 to evaluate vaccine virus replication in the UA. NS were collected using cotton-tipped applicators, placed in 2 ml Leibovitz (L-15) medium with 1x sucrose phosphate (SP) used as a stabilizer and vortexed for 10 seconds. Then aliquots were snap frozen in dry ice and stored at -80°C. Tracheal lavages (TL) were collected after each dose on days -3, 2, 4, 6, 8, 10, 12 and 15 to quantify vaccine virus replication in the LA. TLs were mixed 1:1 with L-15 medium containing 2x SP and aliquots were snap frozen on dry ice and stored at −80°C. Nasal washes (NW) for analysis of mucosal antibodies in the UA were performed on days -3, 15, 21, and 28 using 1 ml of Lactated Ringer's solution per nostril. NW samples were aliquoted, snap frozen on dry ice, and stored at -80°C. Blood was collected on days 0, 15, 21, and 28 pi for analysis of serum antibodies.

METHOD DETAILS

Generation of MPV and derivatives

The recombinant MPV vector backbone used in this study was based on a previously-described MPV reverse genetics system[39] derived from the MPV strain 15 cDNA cloned in a pBluescript vector under control of a T7 promoter.[13] In addition, the downstream 67% of the L ORF were codon-pair optimized for efficient expression in humans.[14] For MPV/S, the full-length 1,273 amino acid (aa) S protein ORF of Wuhan-Hu-1 (GenBank MN908947) was codon optimized for human expression (Genscript) and synthesized commercially (BioBasic). To generate MPV/S-2P, two proline substitutions (aa 986 and 987) were introduced to stabilize S in the prefusion conformation, and four aa mutations (RRAR to GSAS, aa 682-685) were inserted to ablate the furin cleavage site between S1 and S2.[16] S and S-2P inserts were designed so that the ORF was flanked by MPV gene start and gene end transcription signals to enable transcription of S, and the Kozak consensus sequence GCCGCCACC was placed immediately upstream of the S AUG start codon to provide efficient context for translation initiation as previously described.[13] S and S-2P genes were inserted at the third gene position between the MPV NS2 and N genes using XmaI and KpnI restriction sites.

MPV and derivatives were recovered from cDNA as previously described.[13] All *in vitro* tissue culture experiments were done at 32°C unless otherwise noted. In brief, BHK BSR-T7/5 cells that constitutively express the T7 RNA polymerase were transfected using Lipofectamine 3000 with the MPV antigenome plasmid and support plasmids expressing MPV N, P, M2-1, and L proteins. After an overnight incubation at 37°C, the cells were scraped into the media to generate a cell suspension that was co-cultured with a sub-confluent Vero cell monolayer for approximately 2 weeks to generate passage 1 (P1) viral stocks. Virus stocks of MPV and MPV/S were propagated on Vero cells using an MOI $\geq$ 0.01 PFU to generate working virus stocks. Viruses were harvested about 2 weeks post-infection, when cytopathic effects typical for MPV infection disrupted the monolayer. Viruses were further passaged once (MPV) or twice (MPV/S-2P) on Vero cells using an MOI $\geq$0.01 PFU to generate working stocks. Viral RNA was isolated from working stocks using the QIAamp Viral RNA kit (Qiagen), and the genomic sequences were confirmed by Sanger sequencing of overlapping RT-PCR amplicons that covered the whole viral genome with the exception of the regions complementary to the genome-end specific primers (covering 24 and 27 nt of the leader and trailer ends, respectively).

Dual-staining immunoplaque assay

Virus titers were determined by dual-staining immunoplaque assay on Vero cells under a 0.8% methyl cellulose overlay. In brief, tenfold serial dilutions were incubated in duplicate wells on Vero cells under methyl cellulose overlay. After an 11 day incubation at 32°C, monolayers were fixed using 80% methanol, MPV was detected using a rabbit hyperimmune MPV antiserum, and SARS CoV-2 S and S-2P proteins were detected using the human monoclonal antibody CR3022. Anti-rabbit IRDye680 and anti-human IRDye800 infrared fluorophore-labeled secondary antibodies were used to visualize MPV and S, pseudocolored in red and green, respectively, with double-positive plaques appearing yellow/green.

Multicycle kinetics of MPV and derivatives in cell culture

Sub-confluent monolayers of Vero or A549 cells in 12-well plates were infected in duplicate with an MOI of 0.1 PFU/cell of MPV, MPV/S, or MPV/S-2P and incubated at 32°C for 10 days. Vero-grown virus was harvested daily for 10 days, and A549-grown virus was harvested on days 1, 2, 3, 6, 8, and 10 pi. At time of harvest, cells were scraped into the media, vortexed three times for 10 sec each, and centrifuged for 5 min at 850 x g. Clarified supernatants were aliquoted and snap-frozen in dry ice prior to storage at -80°C. The virus titer of each sample was determined by dual-staining immunoplaque assay.

SDS-page and Western blotting

Sub-confluent monolayers of Vero or A549 cells in 12-well plates were infected with an MOI of 2 PFU/cell of MPV, MPV/S, or MPV/S-2P and incubated at 32°C. At 56 hours post infection (hpi), supernatants were removed, and cells were gently washed with 1X PBS before being lysed with 200 μl SDS-PAGE lysis buffer containing protease inhibitors. Cell lysates were clarified using a Qiashredder column (Qiagen) following the manufacturer recommendations and snap-frozen at -80°C until use. NuPAGE Sample Reducing Agent (Thermo Fisher) was added to cell lysates, and proteins were denatured and reduced at 90°C for 10 minutes prior to loading onto 4-15% TGX gels (BioRad). After electrophoresis, proteins were transferred to polyvinylidene difluoride (PVDF) membranes that were next blocked with LiCor blocking buffer for 1 h at room temperature (RT). Then, membranes were incubated at 4°C overnight with 1:25,000 rabbit polyclonal MPV hyperimmune antisera, 1:10,000 mouse polyclonal tubulin antibody (Abcam) and 1:5,000 goat hyperimmune antiserum N25-154, raised against recombinantly-expressed amino acids 1-1208 of the SARS-CoV-2 S-2P protein.[18] After washing five times with PBS supplemented with 0.1% Tween 20, membranes were incubated with infrared-dye labelled secondary antibodies (1:10,000 of donkey anti-rabbit IgG IRDye 680, donkey anti-goat IgG IRDye 800, and donkey anti-mouse IRDye 800, LiCor) at RT for 45 minutes. After incubation, membranes were washed five times with PBS supplemented with 0.1% Tween 20, followed by three washes with PBS before imaging on the Odyssey CLX. Protein bands were quantified using the Image Studio software (LiCor) and normalized to tubulin. Lysates were collected and analyzed in two independent experiments. In each experiment, two wells of a 12-well plate were lysed and analyzed separately.

Sucrose purification of MPV virus stock and derivatives

Aliquots of Vero cell-grown viruses were purified by ultracentrifugation using 30/60% discontinuous sucrose gradients at 134,000 x g for 2 hours at 4°C. Virus particles collected at the 30/60% sucrose interface were diluted in OptiMEM media to decrease the sucrose concentration, snap frozen and stored at -80°C. Prior to analysis, viruses were thawed and centrifuged at 20,000 x g for 2 hours to pellet the virus. Media were removed and virus pellets were resuspended in Tris-EDTA-NaCl (TEN) buffer for measurement of protein content. Protein concentrations were determined using a BCA assay (Pierce Rapid Gold BCA Protein Assay Kit, Thermo Fisher) prior to SDS-PAGE and Western blotting or silver staining (Pierce Silver Stain Kit, Thermo Fisher) using 1 μg of protein per well.

Electron microscopy of sucrose-purified MPV preparations

Two ml of Vero-grown MPV and MPV/S-2P were incubated with 1:100 goat anti-S hyperimmune serum for 40 min at RT with rotation. After incubation, the virus-antibody mixture was transferred to a 30/60% sucrose gradient in 5mL tubes and centrifugated at 160,000 x g at 4°C for 2 h. Purified virus bands at the 30/60% interface were collected and fixed with a final concentration of 2% paraformaldehyde in PBS. Immunogold staining to detect SARS-CoV-2 S was done as previously described.[43] Briefly, 10 μl of purified virus with bound primary antibodies were adsorbed for 30 min to freshly glow-discharged 200 mesh Formvar/carbon-coated Ni grids in saturated humid chambers at RT. Then, grids were washed with PBS, blocked with 2% bovine serum albumin (BSA) in PBS followed by 0.1% acetylated BSA (BSA-c, Aurion) in PBS. All samples were labeled with a donkey anti-goat secondary antibody conjugated to 6 nm gold beads (Aurion) previously diluted 1:50 in 0.1% BSA-c in PBS according to the manufacturer's instructions. Labeled grids were sequentially washed with 0.1% BSA-c in PBS, PBS, and then in water followed by negative-staining with methylamine vanadate and electron microscopy observation.

Replication of MPV and derivatives in the upper and lower airways of macaques

MPV, MPV/S, and MPV/S-2P shedding in the upper and lower airways of macaques was evaluated by dual-staining immunoplaque assay of NS and TL samples collected at the indicated time post-immunization (pi).

Dual IgG and IgA assay to detect anti-S or anti-RBD antibodies

Levels of serum and mucosal IgG and IgA specific to SARS-CoV-2 S protein or its receptor binding domain (RBD) were determined using an IgG/IgA assay designed for detection of antigen-specific IgG by electrochemiluminescence (ECL) ELISA, and antigen-specific IgA, determined in the same assay by a subsequent reading of dissociation-enhanced lanthanide fluorescent (DELFIA) time resolved fluorescence (TRF). In brief, serum and NW samples were heated at 56°C for 30 min to inactivate complement and infectivity. The treated samples were immediately used or stored at -80°C for later use. Black ninety-six–well plates (MaxiSorp, Thermo Fisher Scientific, cat #437111) were coated with 100 μl/well of SARS-CoV-2 S-2P or S-6P (1 μg/ml) or RBD (2 μg/ml)[15,16] in 50 mM carbonate coating buffer [generated by mixing

3.7 g sodium bicarbonate with 0.64 g sodium carbonate (Sigma) in 1 L molecular biology grade water]. After overnight incubation at 4°C, plates were washed three times with washing buffer [PBS (Gibco, cat# 14190-144) containing 0.1% IGEPAL CA-630] using a BioTek 405 micro-plate washer and blocked with 250 μl of blocking buffer [1x DPBS containing 5% dry milk (W/V) (Nestle, Carnation nonfat dry milk)]. After overnight incubation at 4°C, plates were washed one additional time with washing buffer.

Serum or mucosal samples were serially diluted in 96-well plates with a starting dilution at 1:1000 for serum and 1:40 for NW samples, followed by ten 3-fold serial dilutions using sample dilution buffer (PBS+ 5% dry milk+ 0.2% IGEPAL CA-630), leaving column 12 as a blank control. Then, 100 μl of diluted samples were transferred from the dilution plates to the antigen-coated assay plates in duplicate. After incubating for 1 hour at RT on a rotating shaker, plates were washed 3 times with 250 μl washing buffer, and incubated on a rotating shaker for another 20 min. 100 μl per well containing a mix of secondary goat anti-monkey IgG(H+L)-horseradish peroxidase (HRP) conjugated antibody (ThermoFisher, cat# PA1-84631) at 1:10,000 dilution and goat anti-monkey IgA-alpha chain specific Biotin (Alpha Diagnostic International, cat# 70049) at 1:5,000 dilution in dilution buffer, was added, and plates were incubated for 1 h. After incubation with the secondary antibody mix, plates were washed three times and 100 ml per well of Streptavidin-Europium (PerkinElmer, cat# 1244-360) diluted at 1:2,000 in PBS+ 0.2% IGEPAL CA-630 was added. Plates were incubated for 1 h and then washed three times. Then, 50 μl of Pierce ECL HRP substrate (ThermoFisher, cat# 32106) per well was added and after 10 min incubation, plates were read on the Synergy neo (BioTek) plate reader and luminescence data for the IgG detection were collected. After collecting the first set of data, plates were washed three times, and 100 μl per well of pre-warmed DELFIA enhancement solution (PerkinElmer: 4001-0010) was added. Plates were further incubated for 20 min while rocking. After incubation, plates were read again on the Synergy neo (BioTek) plate reader using a program for time-resolved fluorescence (TRF) (using excitation 360/40 and emission 620/40 parameters) and fluorescence data to detect IgA was collected. To measure antigen specific IgG in human plasma samples, a goat anti-human IgG(H+L)-HRP secondary antibody was used at a 1:15,000 dilution in a TMB ELISA.

Finally, data were processed as follows: (i) the average reading for each sample from duplicate wells was calculated, (ii), the average reading from the blank samples was subtracted from the average reading for each sample, (iv) the cut off value was set to the blank average plus three standard deviations of blank readings. Then, the IgG and IgA titers of each sample were determined by interpolating the sigmoid standard curve generated using Prism 9.0.

Serum neutralization assay of SARS-CoV-2 and MPV

Neutralization assays to determine serum antibody titers against SARS-CoV-2 WA1/2020 of immunized macaques were done in a BSL3 laboratory. Sera were heat inactivated at 56°C for 30 min and two-fold serially diluted in Opti-MEM prior to incubation 1:1 with 100 $TCID_{50}$ of SARS-CoV-2 for 1 h at 37°C. Mixtures were added to quadruplicate wells of Vero E6 cells in 96-well plates and incubated for four days. The 50% neutralizing dose (ND_{50}) was the highest dilution of serum that prevented cytopathic effect in 50% of the wells. Serum neutralizing antibody titers against the MPV vector were also quantified on Vero cells using 60% plaque reduction neutralization tests ($PRNT_{60}$).

ACE2 binding inhibition assays

As a complement to the neutralization assay, we evaluated the ability of heat inactivated serum from immunized macaques to inhibit the binding of ACE2 to soluble SARS-CoV-2 spikes (Meso Scale Diagnostics, cat# K15586U, K15609U, and K15671U). Serum samples were diluted 1:20 using the diluent supplied with the kit. Each sample was evaluated in duplicate, and plates were prepared and analyzed as previously described.[44] Briefly, plates in which each well was coated with 10 different soluble spike proteins were blocked for 1h using MSD blocker A buffer followed by a wash with MSD washing buffer. Then, diluted sera were added, and plates were further incubated for 2h on a plate shaker at RT. Sulfo-Tag labelled soluble ACE2 was then added and after 1h incubation, plates were washed. The MSD GOLD electrochemiluminescence read buffer B was next added, and chemiluminescence of bound ACE2-Sulfo-Tag was acquired on a Meso 1300 Quickplex reader. The average electrochemiluminescence signals in duplicate wells for each sample were determined, as well as the maximum electrochemiluminescence signals of ACE2/S protein binding in no-sample control wells. The activity of each serum in blocking ACE2 binding is shown as percent inhibition relative to no-sample controls.

QUANTIFICATION AND STATISTICAL ANALYSIS

Statistics

Data sets were analyzed for significance using One-way ANOVA with Sidak post-test or two-way ANOVA with Tukey post-test on GraphPad Prism version 9.3. A $\log_{10}$ transformation was applied to data sets when necessary to obtain comparable standard deviation among groups of values which is a necessary requirement for these tests. Data sets were only considered significantly different at $p \leq 0.05$.